[CANCER RESEARCH 63, 3567–3574, July 1, 2003]

In Vivo Antitumor Activity of Pegylated Zinc Protoporphyrin: Targeted Inhibition of Heme Oxygenase in Solid Tumor[1]

Jun Fang, Tomohiro Sawa,[2] Takaaki Akaike, Teruo Akuta, Sanjeeb K. Sahoo, Greish Khaled, Akinobu Hamada, and Hiroshi Maeda[3]

Department of Microbiology, Kumamoto University School of Medicine [J. F., T. S., Ta. A., Te. A., S. K. S., G. K., H. M.], and Faculty of Pharmacy, Kumamoto University [A. H.], Kumamoto 860-0811, Japan

ABSTRACT

High expression of the inducible isoform of heme oxygenase (HO-1) is now well known in solid tumors in humans and experimental animal models. We reported previously that HO-1 may be involved in tumor growth (Tanaka *et al.*, Br. J. Cancer, *88:* 902–909, 2003), in that inhibition of HO activity in tumors by using zinc protoporphyrin (ZnPP) significantly reduced tumor growth in a rat model. We demonstrate here that poly(ethylene glycol)-conjugated ZnPP (PEG-ZnPP), a water-soluble derivative of ZnPP, exhibited potent HO inhibitory activity and had an antitumor effect *in vivo*. *In vitro* studies with cultured SW480 cells, which express HO-1, showed that PEG-ZnPP induced oxidative stress, and consequently apoptotic death, of these cells. Pharmacokinetic analysis revealed that PEG-ZnPP-administered i.v. had a circulation time in blood that was 40 times longer than that for nonpegylated ZnPP. More important, PEG-ZnPP preferentially accumulated in solid tumor tissue in a murine model. *In vivo* treatment with PEG-ZnPP (equivalent to 1.5 or 5 mg of ZnPP/kg, i.v., injected daily for 6 days) remarkably suppressed the growth of Sarcoma 180 tumors implanted in the dorsal skin of ddY mice without any apparent side effects. In addition, this PEG-ZnPP treatment produced tumor-selective suppression of HO activity as well as induction of apoptosis. The major reason for tumor-selective targeting of PEG-ZnPP is attributed to the enhanced permeability and retention effect that is observed commonly in solid tumors for biocompatible macromolecular drugs. These findings suggest that tumor-targeted inhibition of HO activity could be achieved by using PEG-ZnPP, which induces apoptosis in solid tumors, probably through increased oxidative stress.

INTRODUCTION

HO[4] catalyzes the rate-limiting step in the degradation of heme to produce biliverdin, CO, and free iron. Thus, Biliverdin formed is subsequently converted to bilirubin by cytosolic biliverdin reductase (1, 2). The constitutive isoform of HO (HO-2) is highly expressed in the testis and brain under physiological conditions (2). HO-1, an inducible isoform of HO, is found at low levels in most mammalian tissues but is highly expressed in liver and spleen (3). Expression of HO-1 is induced by a wide variety of stress-inducing stimuli, including heat shock (4), UV irradiation (5), hydrogen peroxide (5), heavy metals (5, 6), hypoxia (7), and NO (8, 9). Bilirubin has been reported to behave as an antioxidant by scavenging free radicals (10–12). CO has also been shown to provide protection of cells against injury of various kinds both *in vitro* and *in vivo* (13, 14).

HO-1 may serve as a key biological molecule in the adaptation to and/or defense against oxidative stress and cellular stress. It is interesting to note that several tumors, including renal cell carcinoma (15) and prostate tumors (16) in humans, express a high level of HO-1. We also found high HO-1 expression in experimental solid tumors, *i.e.*, the rat hepatoma AH136B (9) and the mouse sarcoma Sarcoma 180 (17). This level of HO-1 expression was comparable with that in the spleen and liver (9, 17). In these models, inducible NO synthase was also up-regulated, and, thus, tumor tissues were exposed to oxidative stress related to NO and/or its reactive metabolites (18, 19). Administration of the HO inhibitor ZnPP via a tumor-feeding artery significantly suppressed the growth of AH136B tumors, which suggests a vital role of HO-1 in tumor growth (9). These findings also indicate a potential beneficial role of HO inhibitors as novel anticancer agents. However, the mechanism of *in vivo* antitumor activity of HO inhibitors developed thus far has not yet been fully proved.

Metalloporphyrins constitute a class of compounds in which the central iron of heme is replaced by various other metals such as cobalt, zinc, manganese, chromium, or tin (20). These metalloporphyrins function as competitive inhibitors of the HO reaction because of their inefficient binding to molecular oxygen, which prevents HO from degrading the metalloporphyrins (20). Although these metalloporphyrins may exhibit antitumor activity, as has been shown for ZnPP, their extremely low solubility in water limits additional investigation of these compounds *in vivo*. To overcome this limitation, we recently developed a water-soluble derivative of ZnPP by conjugating it with a water-soluble polymer, PEG (17). This polymer conjugate PEG-ZnPP was not only active as a HO inhibitor, similar to native ZnPP, but also behaved as a macromolecular agent because of its micelle formation (17). Furthermore, i.v. injection of PEG-ZnPP significantly reduced intratumor HO activity. In the present study, *in vivo* antitumor activity of PEG-ZnPP was demonstrated by using a murine solid tumor model. Pharmacokinetics and side effects of PEG-ZnPP treatment were also examined.

MATERIALS AND METHODS

Materials. Protoporphyrin IX was purchased from Sigma Chemical Co. (St. Louis, MO). The succinimidyl derivative of PEG (MEC-50HS), which reacts with a primary amino group (21), with an average molecular weight of 5000, was kindly provided by NOF Co. (Tokyo, Japan). Other reagents were of reagent grade and were used without further purification.

Animals. Male ddY mice, 6 weeks old and each weighing 30–35 g, were from SLC, Inc. (Shizuoka, Japan). All of the experiments were carried out according to the guidelines of the Laboratory Protocol of Animal Handling, Kumamoto University School of Medicine.

Synthesis of PEG-ZnPP. The synthesis, purification, and characterization of PEG-ZnPP were described in our recent work (17).

Cell Culture. Human colon cancer SW480 cells were cultured in DMEM supplemented with 10% FCS at 37°C in a 5% CO_2-95% air atmosphere. Mouse

Received 12/26/02; accepted 5/8/03.

The costs of publication of this article were defrayed in part by the payment of page charges. This article must therefore be hereby marked *advertisement* in accordance with 18 U.S.C. Section 1734 solely to indicate this fact.

[1] Supported in part by Grant-in-Aid from the Ministry of Education, Culture, Sports, Science and Technology of Japan (No. 13218107).

[2] Present address: Unit of Endogenous Cancer Risk Factors, IARC, Cours Albert Thomas, 69372 Lyon, France.

[3] To whom requests for reprints should be addressed, at Department of Microbiology, Kumamoto University School of Medicine, Honjo 2-2-1, Kumamoto 860-0811, Japan. Phone: 81-96-373-5098; Fax: 81-96-362-8362; E-mail: msmaedah@gpo.kumamoto-u.ac.jp.

[4] The abbreviations used are: HO, heme oxygenase; ZnPP, zinc protoporphyrin; PEG, poly(ethylene glycol); ROS, reactive oxygen species; NO, nitric oxide; CO, carbon monoxide; NAC, *N*-acetylcysteine; DCDHF, 2′,7′-dichlorodihydrofluorescein; EPR, enhanced permeability and retention; AUC, area under the concentration *versus* time curve; TUNEL, terminal deoxynucleotide transferase (TdT)-mediated dUTP-biotin nick end-labeling; RES, reticuloendothelial system; RT-PCR, reverse transcription-PCR; MTT, 3-(4,5-dimethylthiazol-2-yl)-2,5-diphenyltetrazolium bromide; TNF, tumor necrosis factor; siRNA, small interfering RNA; G3PDH, glyceraldehyde-3-phosphate dehydrogenase; PEG-PP, poly(ethylene glycol)-conjugated protoporphyrin IX.

sarcoma Sarcoma 180 cells were maintained by passage i.p. in ddY mice, and, thus, cells obtained as ascitic-free floating cells were used after washing.

RT-PCR Assay for Expression of HO-1 mRNA in SW480 Cells. Total RNA from SW480 cells was extracted by using TRIzol reagent (Life Technologies, Inc., Grand Island, NY), according to the manufacturer's instruction. The RT-PCR assay to detect HO-1 expression was performed according to the method reported by Abraham (22). The cDNA product obtained by reverse transcription with random primers was amplified by PCR. The nucleotide sequences of the oligonucleotide primers used for PCR are as follows: HO-1 antisense 21-mer, 5′GATGTTGAGCAGGAACGCGAT′; and HO-1 sense 21-mer, 5′CAGGCAGAGAATGCTGAGTTC′ to obtain a 555-bp HO-1 cDNA (nucleotides 79–633 of the coding sequence). In some experiment, an antisense primer 5′AATCTTGCACTTTGTTGCTGG′ was used to yield 662-bp HO-1 cDNA fragment (nucleotides 79–740 of the coding sequence). After an initial denaturing step at 94°C, 25 PCR cycles were performed as follows: denaturing for 1 min at 94°C, primer annealing for 1 min at 56°C, and DNA synthesis for 1 min at 72°C. The mRNA for G3PDH was examined as a standard mRNA expressed in the cells in the same manner as for HO-1, except that 30 PCR cycles were used. The nucleotide sequences of the primer for RT-PCR for G3PDH are as follows: antisense 24-mer, 5′CATGTGGGCCATGAGGTCCACCAC3′ and sense 26-mer, 5′TGAAGGTCGGAGTCAACGGATTTGGT3′ to obtain a 983-bp G3PDH cDNA fragment. PCR products then underwent electrophoresis on ethidium bromide-stained 1% agarose gels.

MTT Assay. *In vitro* cytotoxicity of PEG-ZnPP was determined by the MTT assay (23). Cells were seeded in 96-well culture plates (3000 cells/well), and after an overnight preincubation, cells were exposed to indicated concentrations of PEG-ZnPP for 48 h. The toxicity of PEG-ZnPP was expressed as the fraction of cells surviving relative to untreated controls.

Induction of Oxidative Stress by PEG-ZnPP. SW480 cells were seeded in 12-well plates (10^5 cells/well). After an overnight preincubation, cells were treated with PEG-ZnPP for 8 h. Then, 10 μM DCDHF-diacetate was added, and the cells were cultured for an additional 30 min. The esterified form of DCDHF-diacetate can permeate cell membranes and then be deacetylated by intracellular esterases. The resultant compound, DCDHF, reacts with ROS to give a fluorescent compound, dichlorofluorescein, which remains in the cells (24). The amount of intracellular ROS was quantitated as a function of fluorescence intensity measured by flow cytometry (BD FACSCalibur 3A; Becton Dickinson, San Jose, CA).

***In Vitro* Apoptosis Assay.** Proapoptotic activity of PEG-ZnPP was determined by a flow cytometric assay with Annexin V-FITC (25), by using the Annexin V-FITC Apoptosis Detection kit (BD PharMingen, San Diego, CA). In brief, SW480 cells plated in 12-well plates (10^5 cells/well) were preincubated overnight. Then, cells were treated with PEG-ZnPP for 24 or 48 h. After the cells were harvested by use of a rubber policeman, they were subjected to staining with the Annexin V-FITC kit and propidium iodide. The number of apoptotic cells was determined by flow cytometry (BD FACSCalibur 3A).

To study the effect of HO inhibition on induction of apoptosis, HO-1 expression was specifically suppressed by using a 21-nucleotide duplex siRNA (26), which targets nucleotides 612–630 of the HO-1 mRNA coding sequence. The sequences of ribonucleotides used were 5′-rGACUGCGUUCCUGCUCAACdTdT-3′ and 5′-rGUUGAGCAGGAACGCAGUCdTdT-3′ (Dharmacon Research Inc., Lafayette, CO). SW480 cells (10^5 cells/well) were plated in six-well plates and were preincubated overnight, after which 2 μg of siRNA was introduced into the cells by use of TransMessenger Transfection Reagent according to the manufacturer's directions (Qiagen GmbH, Hilden, Germany). Forty-eight h after transfection, cells were harvested and subjected to the apoptosis assay described above. At the same time, the effect of siRNA treatment on the HO-1 expression of the cells was examined by RT-PCR for HO-1 mRNA as described above.

Determination of Pharmacokinetics of PEG-ZnPP after i.v. Injection into ddY Mice. *In vivo* pharmacokinetics of PEG-ZnPP were examined by use of its ^{65}Zn-labeled derivatives and were compared with that of native, nonpegylated ZnPP. Radiolabeled PEG-ZnPP was prepared by the same method as that described by Sahoo *et al.* (17), in which ^{65}Zn-labeled zinc acetate (Perkin-Elmer Japan Co. Ltd., Yokohama, Japan) was used. Radiolabeled native ZnPP was obtained by incorporation of ^{65}Zn to protoporphyrin IX in DMSO. Free ^{65}Zn in the preparations of PEG-ZnPP and native ZnPP was removed by gel chromatography with a Sephadex G-25 column (PD-10 columns; Amersham Pharmacia Biotech AB, Uppsala, Sweden) and by dialysis against distilled water, respectively. Mouse sarcoma Sarcoma 180 cells (2×10^6 cells) were implanted s.c. in the dorsal skin of ddY mice. The study of the body distribution of PEG-ZnPP was performed on days 7–10 after tumor inoculation, when tumors were 5–7 mm in diameter and had no necrotic region.

Mice received i.v. injections of ^{65}Zn-labeled PEG-ZnPP or native ZnPP via the tail vein [0.3 mM, 15,000 cpm (0.33 kBq)/mouse, 0.1 ml/injection]. After scheduled time, mice were killed, blood samples were drawn from the inferior vena cava, and mice were then subjected to reperfusion with 10 ml of saline containing heparin (5 units/ml) to remove blood components in the blood vessels of the tissues. Then, tumor tissues as well as normal tissues, including liver, spleen, kidney, intestine, heart, lung, brain, and muscle, were collected and weighed. Radioactivity of these tissues was measured by using a gamma counter (Wallac 1480 WIZARD 3"; Pharmacia Biotech, Turku, Finland).

Assay of *In Vivo* Antitumor Activity of PEG-ZnPP. Another group of ddY mice, implanted with Sarcoma 180 tumor cells as just described, was used to examine the antitumor activity of PEG-ZnPP. Tumor-bearing mice were treated with the reagents of interest at 7 days after tumor inoculation, when tumors had achieved to a diameter of 4–5 mm. PEG-ZnPP (1 or 3 mM, 0.1 ml) was administered (equivalent to 1.5 or 5 mg of ZnPP/kg) i.v., daily for 6 days. In control experiments, mice received physiological saline (0.1 ml) instead of the PEG-ZnPP solution. The tumor volume and body weight of the mice were measured daily during the period of investigation. Values for the tumor volume (V) were determined by measuring the longitudinal cross section (L) and the transverse section (W) and then applying the formula $V = (L \times W^2)/2$.

Measurement of HO Activity. Tumor, spleen, and liver tissues collected from mice with or without the above-described PEG-ZnPP treatment were homogenized by a Polytron homogenizer with ice-cold homogenate buffer [20 mM potassium phosphate buffer (pH 7.4) plus 250 mM sucrose, 2 mM EDTA, 2 mM phenylmethylsulfonyl fluoride, and 10 μg/ml leupeptin]. Homogenates were centrifuged at 10,000 $\times$ *g* for 30 min at 4°C, after which the resultant supernatant was ultracentrifuged at 105,000 $\times$ *g* for 1 h at 4°C. The microsomal fraction was suspended in 0.1 M potassium phosphate buffer (pH 7.4) followed by sonication for 2 s at 4°C. The reaction mixture that was used for measurement of HO activity was composed of microsomal protein (1 mg), cytosolic fraction of rat liver (1 mg of protein) as a source of biliverdin reductase, 33 μM hemin, and 333 μM NADPH in 1 ml of 90 mM potassium phosphate buffer (pH 7.4). The mixture was incubated for 15 min at 37°C, at which point the reaction was terminated by the addition of 33 μl of 0.01 M HCl. The bilirubin formed in the reaction was extracted with 1 ml of chloroform, and the bilirubin concentration was determined spectroscopically by measuring the difference in absorbance between 465 and 530 nm, with a molar extinction coefficient of 40 mM^{-1} cm^{-1}.

Western Blot Analysis of HO-1 Expression. The microsomal fraction obtained as just described was used for analysis of HO-1 expression. Total protein (25 μg in each sample) in tissue homogenates was separated by electrophoresis with 12% SDS-polyacrylamide gels and was transferred to Immobilon polyvinylidene difluoride membranes (Millipore Co., Ltd., Bedford, MA). This process was followed by reaction with a polyclonal antibody to HO-1 (OSA-150; Stressgen, Victoria, British Columbia, Canada). The protein band that reacted immunologically with the antibody was visualized by using the enhanced chemiluminescence system (Amersham International plc, Buck, United Kingdom), combined with chemiluminescence detection with Hyperfilm (Amersham).

Determination of Blood Count and Blood Chemistry. Mice bearing Sarcoma 180 tumors about 5–7 mm in diameter were used for this study. Twenty-four h after PEG-ZnPP treatment as described above, mice were killed and blood samples were obtained from the inferior vena cava. RBC, WBC counts, and hemoglobin levels were determined by routine clinical laboratory techniques (27). Plasma obtained by centrifugation was used for measurement of alanine aminotransferase, aspartate aminotransferase, lactate dehydrogenase, blood urea nitrogen, and creatinine values by using a sequential multiple AutoAnalyzer system (Hitachi Ltd., Tokyo, Japan).

ELISA of TNF-α in Mice Treated by PEG-ZnPP. At 24 h and 3 days after the above-mentioned 6-day PEG-ZnPP treatment, the TNF-α levels in sera of mice were quantitated *in vitro* by use of a mouse TNF-α ELISA kit (BioSource International, Inc., Camarillo, CA), according to the manufacture's instruction.

***In Situ* Apoptosis Detection.** As described earlier, tumor, liver, and kidney were collected after reperfusion of the mice with 10 ml of physiological saline containing heparin (5 units/ml), and were used for the apoptosis assay and for the histological examination that is discussed below. *In vivo* induction of apoptosis by PEG-ZnPP treatment was determined by the TUNEL method (28), with an *in situ* apoptosis detection kit (TACS; Trevigen Inc., Gaithersburg, MD), according to the manufacturer's instruction. Tissue specimens from the mice were embedded in an embedding dish (Greiner Bio-one Co., Ltd., Tokyo, Japan) by using Tissue-Tek OCT Compound (Sakura Finetechnical Co., Ltd., Tokyo, Japan) and were stored at −80°C before use. Cryosections (10-μm thick) were prepared for this assay. Serial sections were used for the TUNEL assay. TUNEL-positive cells were counted in four different fields per sample, and counts were expressed per mm^2 of tissue section.

Histological Examination. Some tissue specimens collected as described above were fixed with 10% buffered neutral formalin solution and were then embedded in paraffin. Sections were stained with H&E.

Statistical Analysis. All of the data are expressed as means ± SE. Student's *t* test was used to determine the significance between each experimental group. The difference was considered statistically significant when $P < 0.05$.

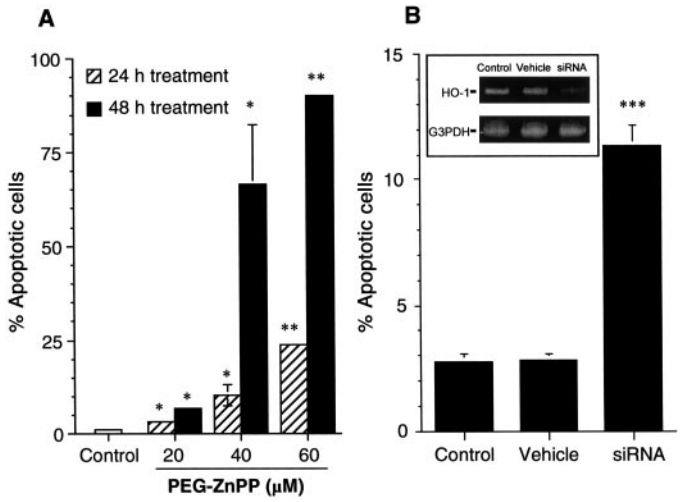

Fig. 3. Induction of apoptosis in SW480 cells by PEG-ZnPP. Cells were treated with increasing concentrations of PEG-ZnPP for 24 h or 48 h (*A*) or with siRNA for 48 h (*B*). The number of apoptotic cells was determined by flow cytometry, and the percentage of apoptotic cells (per the total number of calculated cells) is shown. Values are means ($n = 3$ wells); *bars*, ±SE. In *A*, $*P < 0.05$ and $**P < 0.00001$ *versus* control. In *B*, vehicle indicates the result for cells treated with TransMessenger Transfection Reagent only (without siRNA); siRNA indicates the result for cells transfected with siRNA for HO-1 mRNA; $***P < 0.0007$ *versus* control (no treatment). The *inset* in *B* shows RT-PCR analyses for the HO-1 mRNA expression of the cells with or without siRNA (or vehicle) transfection.

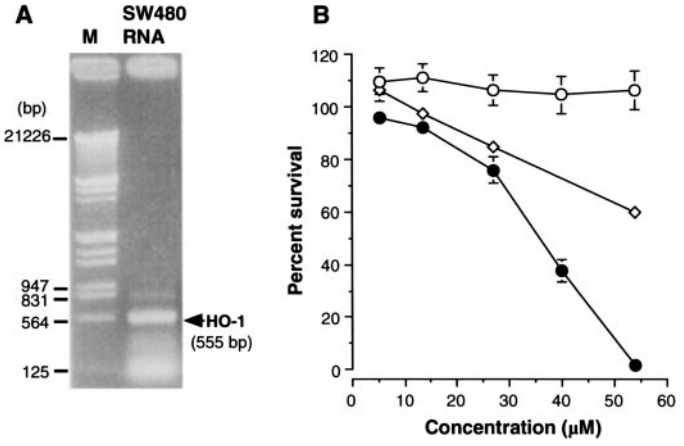

Fig. 1. *In vitro* cytotoxicity of PEG-ZnPP. *A*, RT-PCR detection of HO-1 mRNA expressed in SW480 cells. *M*, molecular size markers; *SW480 RNA*, total RNA extracted from SW480 cells. *B*, cytotoxicity of PEG-ZnPP. SW480 cells were exposed to increasing concentrations of PEG-ZnPP or PEG-PP for 48 h. Other SW480 cells were incubated with PEG-ZnPP in the presence of NAC (2 mM). Cell viability was then determined by the MTT assay. ●, PEG-ZnPP; ○, PEG-PP; ◇, PEG-ZnPP plus NAC. Values are means ($n = 6$ wells); *bars*, ±SE.

RESULTS

***In Vitro* Cytotoxicity of PEG-ZnPP as Related to Increased Oxidative Stress.** SW480 cells cultured *in vitro* did express HO-1 mRNA, as demonstrated by RT-PCR (Fig. 1*A*). As shown in Fig. 1*B*, PEG-ZnPP, at concentrations of 5.4–54.0 μM, exhibited a cytotoxic effect in a dose-dependent manner. This cytotoxic effect was largely reversed by addition of the antioxidant, NAC (at 2 mM, NAC itself resulted in the cell viability of 105.8 ± 5.8% compared with untreated control), which suggests the involvement of increased oxidative stress in the cytotoxic action of PEG-ZnPP. In addition, PEG-PP, a metal-free analogue of PEG-ZnPP that does not inhibit HO, had no cytotoxic effect at the same concentration range (Fig. 1*B*).

To investigate whether PEG-ZnPP increases the intracellular production of ROS in SW480 cells, flow cytometry was performed with the use of the oxidant-sensitive fluorescence probe DCDHF (24). As shown in Fig. 2, PEG-ZnPP increased the fluorescence intensity of cells in a dose-dependent manner, whereas PEG-PP did not. These

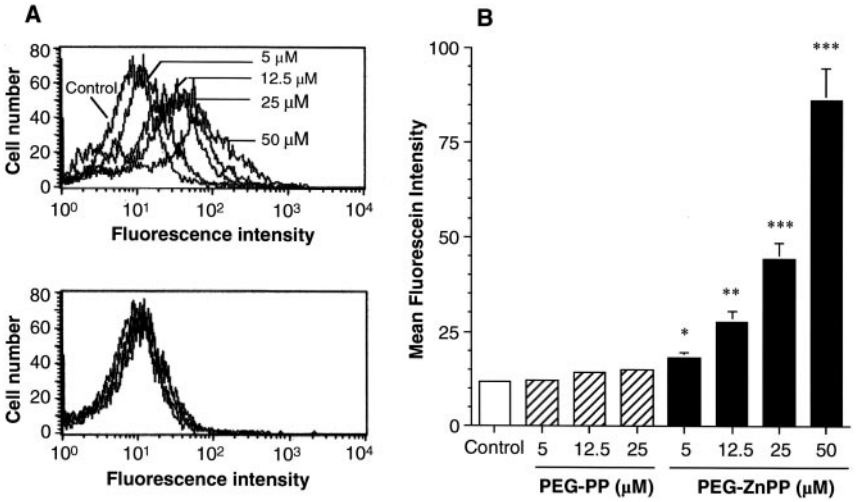

Fig. 2. Induction of intracellular ROS production in SW480 cells by treatment with PEG-ZnPP. SW480 cells were treated with increasing concentrations of PEG-ZnPP or PEG-PP for 8 h. The amount of intracellular ROS was measured by flow cytometry. Values are means ($n = 3$ wells). $*P < 0.01$, $**P < 0.005$, $***P < 0.002$, PEG-ZnPP *versus* control; *bars*, ±SE.

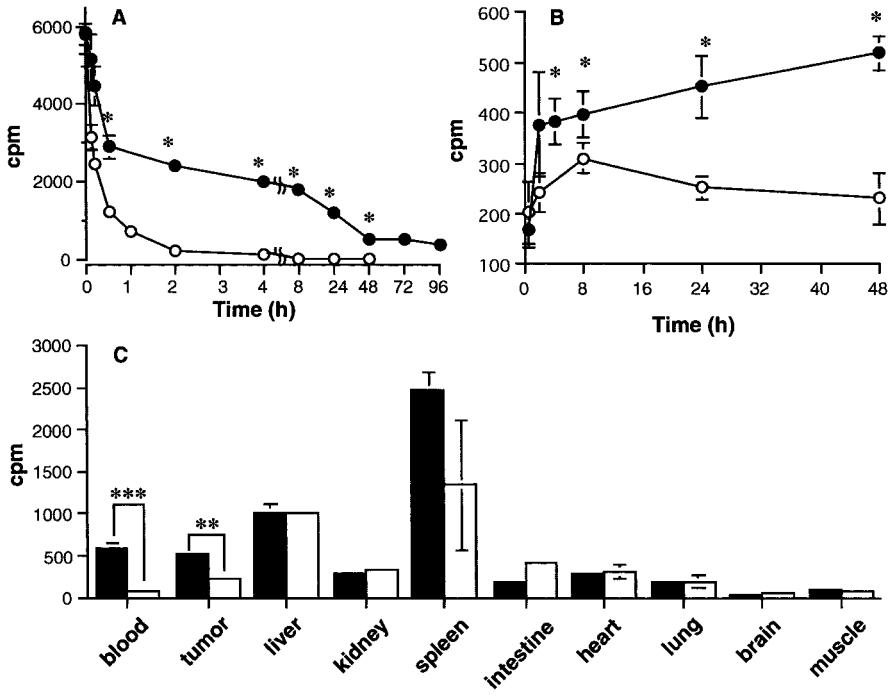

Fig. 4. Pharmacokinetics of PEG-ZnPP and native ZnPP in ddY mice bearing Sarcoma 180 tumor as determined by using radioactive derivatives. Radiolabeled native ZnPP or PEG-ZnPP was injected i.v. into tumor-bearing mice. After scheduled time periods, mice were killed, and samples of blood, tumor, and normal tissues and organs were collected. Radioactivity of each tissue or organ was then measured. *A*, plasma level of PEG-ZnPP (●) and native ZnPP (○). *B*, tumor accumulation of PEG-ZnPP (●) and native ZnPP (○). *C*, body distribution of native ZnPP (□) and PEG-ZnPP (■) 48 h after i.v. injection. Results (*A–C*) are expressed as means; *bars*, ±SE ($n = 3$ or 4). $*P < 0.01$, $**P < 0.005$, $***P < 0.0005$, PEG-ZnPP *versus* native ZnPP.

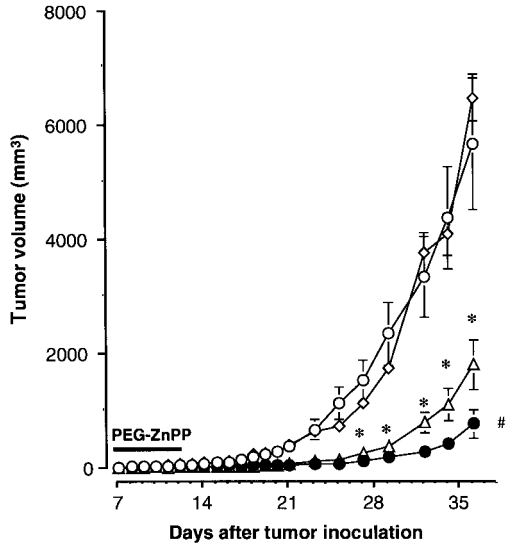

Fig. 5. Antitumor effect of PEG-ZnPP in the Sarcoma 180 solid tumor model. Sarcoma 180 cells (2×10^6 cells) were implanted s.c. in ddY mice. Seven days later, mice were treated with different doses of PEG-ZnPP (●, 5 mg/kg; △, 1.5 mg/kg) or PEG-PP (◇, 5 mg/kg) daily for 6 days. Control mice (○) received injections of physiological saline. Data are means ($n = 6–8$); *bars*, ±SE. $*P < 0.001$ PEG-ZnPP groups *versus* PEG-PP and control groups. #, complete regression of tumor growth was observed in two of eight tumors after treatment with PEG-ZnPP (5 mg/kg).

findings suggest that the increased oxidative stress was because of inhibition of HO activity.

PEG-ZnPP-induced Apoptosis in SW480 Cells. To investigate whether apoptosis is involved in the cytotoxic action of PEG-ZnPP, a fluorescein-labeled Annexin V assay was performed to detect apoptotic SW480 cells after PEG-ZnPP treatment. PEG-ZnPP induced apoptosis in these cells in a concentration-dependent manner (Fig. 3*A*). This result correlated well with the increase in formation of intracellular oxidant as shown in Fig. 2*B*. More important, very little necrosis was found on this treatment. In 24-h treatment, necrosis were found to be <1% of total counted cells in all of the groups; the necrosis observed in 48-h treatment were 0.18%, 0.32%, 1.1%, and 1.76% of total counted cells for the control, PEG-ZnPP 20 μM, 40 μM, and 60 μM groups, respectively. These results suggest that the cytotoxicity of PEG-ZnPP is mostly because of induction of apoptosis.

Targeted knockdown of HO-1 expression was achieved by transfection of siRNA, which, thus, induced apoptosis of cultured SW480 cells (Fig. 3*B*). Suppression of HO-1 levels after siRNA treatment was confirmed by RT-PCR analysis for HO-1 mRNA of the cells as shown in the inset of Fig. 3*B*. This finding indicates that HO-1 plays an important role in preventing apoptosis of SW480 cells under the study conditions. Thus, PEG-ZnPP-induced inhibition of HO activity results in apoptosis through a mechanism involving the increased oxidative stress.

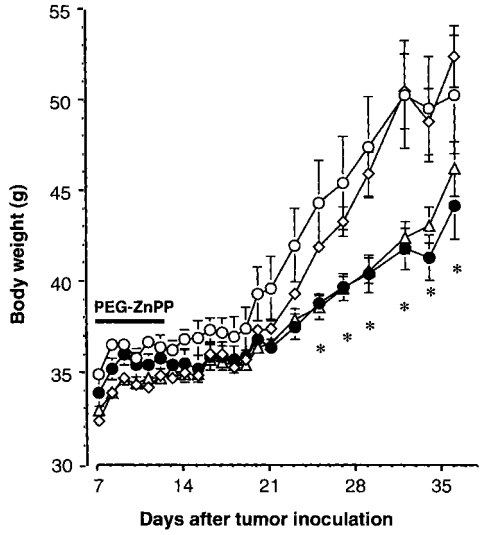

Fig. 6. Body weight changes of ddY mice treated with PEG-ZnPP. The treatment protocol was the same as that described for Fig. 5. ○, control mice bearing Sarcoma 180 tumor, no drug treatment; ●, 5 mg/kg PEG-ZnPP; △, 1.5 mg/kg PEG-ZnPP; ◇, 5 mg/kg PEG-PP. The body weight change of mice without tumor was similar to that of group ● and △ (data not shown). Data are mean ($n = 3$ or 4); *bars*, ±SE. $*P < 0.05$ for group ● and ◇ compared with the control and PEG-PP groups.

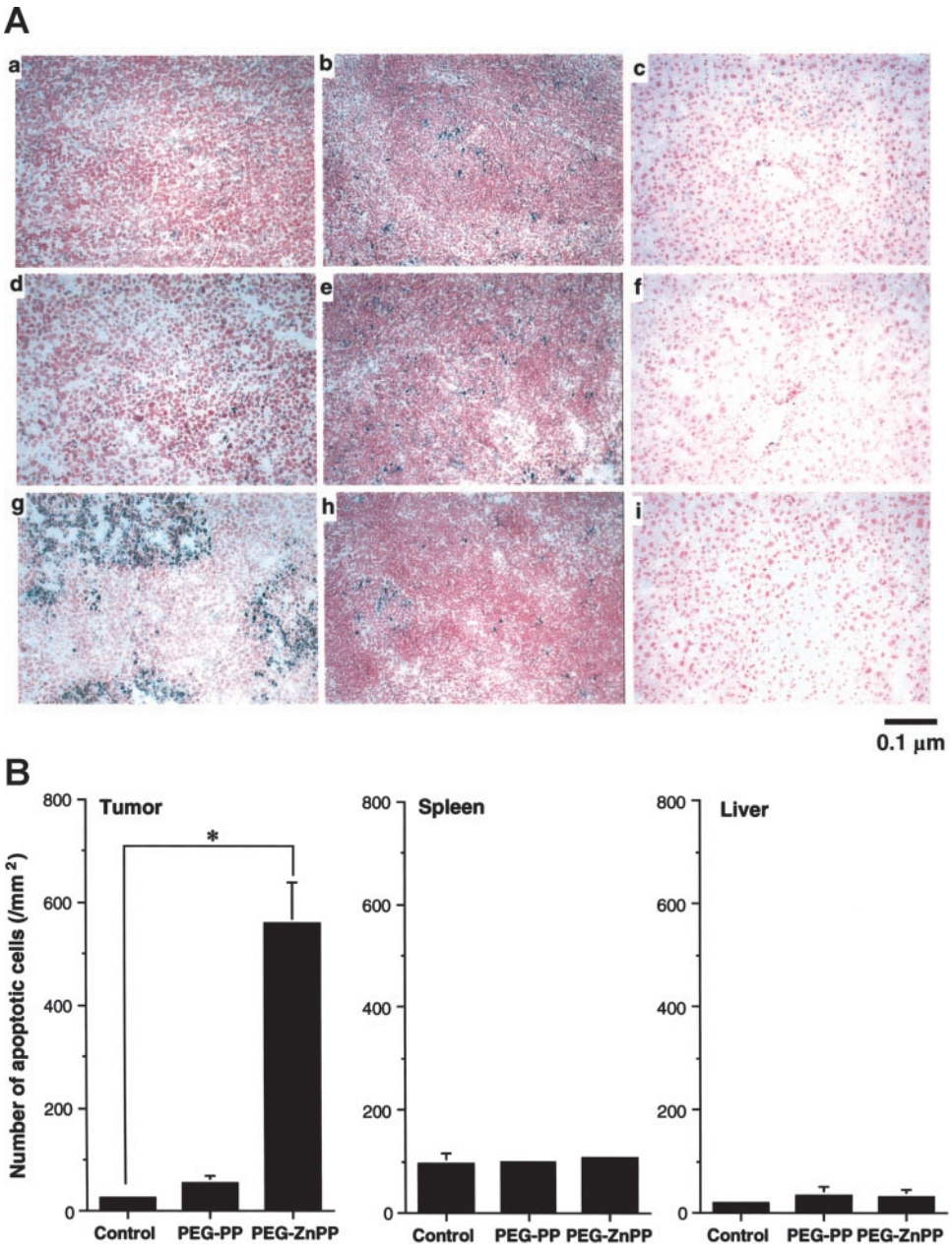

Fig. 7. Induction of apoptosis in Sarcoma 180 solid tumors by PEG-ZnPP. Each specimen was collected and examined 24 h after treatment. The treatment protocol was the same as that described for Fig. 5. *A*, TUNEL staining for each group: *a*, *d*, *g*, tumor; *b*, *e*, *h*, spleen; *c*, *f*, *i*, liver. *a*, *b*, *c*, untreated controls; *d*, *e*, *f*, PEG-PP; *g*, *h*, *i*, PEG-ZnPP. Apoptosis exhibits a dark blue staining. Morphometric analyses of the number of TUNEL-positive cells in each specimen are shown in *B*. TUNEL-positive cells were counted in four different fields per sample, and counts were calculated as the number of positive cells per mm^2. Data are means ($n = 3$ for each group); *bars*, ±SE. $*P < 0.005$, PEG-ZnPP group *versus* control and PEG-PP groups.

Pharmacokinetics of PEG-ZnPP after i.v. Injection. As shown in Fig. 4*A*, nonpegylated native ZnPP rapidly disappeared from the blood circulation after i.v. injection; the AUC was 2,505 ± 396 (cpm·h)/ml. In contrast, PEG-ZnPP showed a significantly longer circulation time. An AUC value that was >40 times higher [102,290 ± 11,649 (cpm·h)/ml] was achieved by PEG-ZnPP.

It is important to note that in tumor tissue PEG-ZnPP accumulated in a time-dependent manner, with a maximum increase at 48 h, whereas native ZnPP reached a maximum accumulation at 8 h after administration and then gradually disappeared (Fig. 4*B*).

Body distribution analysis showed a PEG-ZnPP buildup in the liver and the spleen, both of which have an active RES (29). This observation suggests that PEG-ZnPP after systemic administration is trapped by the RES. Besides the liver and spleen, tumor tissue showed a PEG-ZnPP accumulation greater than that in other normal tissues (Fig. 4*C*), which suggests a preferential concentration of PEG-ZnPP in tumor.

***In Vivo* Antitumor Activity of PEG-ZnPP.** As shown in Fig. 5, tumor growth was significantly suppressed in mice receiving PEG-ZnPP treatment. With the dose of 5 mg/kg, tumor growth was continuously suppressed until at least 36 days after tumor implantation, which was 24 days after the last administration of PEG-ZnPP. Complete regression of tumor growth was observed in two of eight tumors after treatment with PEG-ZnPP (5 mg/kg). In contrast, in mice treated with PEG-PP, tumor growth was not delayed. In addition, the effect of native ZnPP was not examined in this *in vivo* antitumor study, because it is not soluble in water at the dose mentioned above, which is not suitable for systemic administration. The average tumor weights on the 36th day after tumor implantation for the groups treated with the high dose of PEG-ZnPP (5 mg/kg), the low dose of PEG-ZnPP (1.5 mg/kg), or PEG-PP and for the untreated control group were 1.43 ± 0.36, 2.17 ± 0.39, 7.04 ± 0.98, and 6.14 ± 1.03 g, respectively.

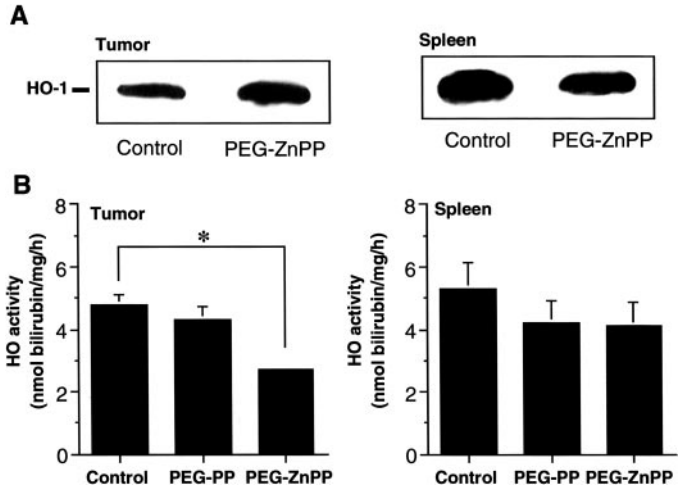

Fig. 8. Modulation by PEG-ZnPP of HO-1 expression (*A*) and activity (*B*) in the Sarcoma 180 solid tumor model. Tumor-bearing ddY mice were treated with PEG-ZnPP according to the same protocol as that described for Fig. 5. Twenty-four h after the last injection, tumors and spleens were obtained and were used for (*A*) Western blotting for HO-1 protein and (*B*) HO activity after PEG-ZnPP treatment. Values are means ($n = 4$); *bars*, ±SE. $*P < 0.005$, PEG-ZnPP group *versus* control group ($P < 0.03$, PEG-ZnPP group *versus* PEG-PP group).

Body Weight Changes after PEG-ZnPP Treatment. Fig. 6 shows body weight changes of mice receiving different treatments. Early in the observation period, no group showed a loss of body weight. However, during the later stage of investigation, a significant difference in body weight was observed in the groups treated with PEG-ZnPP compared with the nontreated control group and the PEG-PP-treated group. This body weight change is attributed primarily to the difference in tumor weight among these groups, as mentioned above.

***In Vivo* Induction of Tumor Cell Apoptosis of PEG-ZnPP.** The TUNEL assay was used to examine apoptosis induced *in vivo* by PEG-ZnPP. Untreated control and PEG-PP-treated specimens showed only negligible positive staining, whereas strong positive staining was observed in PEG-ZnPP-treated Sarcoma 180 tumor tissue (Fig. 7*A*). Morphometric analysis of TUNEL-positive cells in the Sarcoma 180 solid tumors showed that the numbers of positive cells in the control group, the PEG-PP-treated group, and the 5 mg/kg PEG-ZnPP-treated group were 25.9 ± 5.7, 55.5 ± 14.9, and 560.5 ± 77.3/mm^2, respectively (Fig. 7*B*). In contrast, no significant increase in apoptosis was found after PEG-ZnPP treatment in the liver and spleen (Fig. 7).

Targeted Inhibition by PEG-ZnPP of HO Activity in Sarcoma 180 Solid Tumor. To clarify whether the induction of apoptosis *in vivo* and thus the suppression of tumor growth caused by PEG-ZnPP were because of the inhibition of HO activity, the expression and activity of HO-1 in tumor and spleen after PEG-ZnPP treatment were examined. As shown in Fig. 8*A*, HO-1 protein was clearly expressed in tumor and spleen of ddY mice. More important, even though HO-1 protein increased in tumor after PEG-ZnPP treatment (Fig. 8*A*), this treatment significantly inhibited (by ~50%) HO activity in the tumor (Fig. 8*B, tumor*). In contrast, PEG-ZnPP treatment neither increased HO-1 protein nor inhibited HO activity in the spleen (Fig. 8*B, spleen*). Similarly, HO activity in liver was not affected by PEG-ZnPP treatment (data not shown).

Evaluation of Side Effects of PEG-ZnPP Treatment. Because of a report that ZnPP is potentially toxic to both myeloid and erythroid cell growth (30), the hematological toxicity of PEG-ZnPP treatment was investigated in Sarcoma 180 tumor-bearing mice, by blood cell measures (RBC, WBC, and hemoglobin). No significant decreases in RBC and WBC counts, and hemoglobin levels were found after PEG-ZnPP treatment at the dose effective against cancer, compared with the measures in untreated control (Table 1). In addition, no significant effects of PEG-ZnPP treatment were seen in biochemical assays of major organs (liver and kidney), *i.e.*, plasma alanine aminotransferase, aspartate aminotransferase, lactate dehydrogenase, blood urea nitrogen, and creatinine values (Table 1).

HO-1 has also been known to be anti-inflammatory in various settings (31–33). To additionally clarify whether inhibition of HO-1 by PEG-ZnPP will induce spontaneous inflammation, the proinflammatory cytokine TNF-α was measured by use of a mouse TNF-α ELISA for evaluating systemic inflammation in mice receiving PEG-ZnPP treatment. Either at 24 h or 3 days after PEG-ZnPP treatment, no increment of TNF-α production in sera of mice with PEG-ZnPP treatment was observed compared with untreated control mice. The levels of TNF-α in all of the serum samples measured (both control and PEG-ZnPP treatment groups) were <19.5 pg/ml (detection limit of this ELISA).

Histological Examination. Tumor tissues showed necrotic changes, whereas no pathological changes were observed in the liver and spleen, after PEG-ZnPP treatment (data not shown).

DISCUSSION

The present study investigated the antitumor activity of a water-soluble HO inhibitor, PEG-ZnPP. *In vitro* experiments showed that PEG-ZnPP had cytotoxic effects on cultured SW480 cells, which express HO-1, whereas PEG-PP, a zinc-free analogue of PEG-ZnPP having no HO inhibitory activity, did not (Fig. 1). Coincubation of cells with the antioxidant NAC reduced the cytotoxicity of PEG-ZnPP. In addition, flow cytometric analysis using an oxidant-sensitive fluorescence probe (DCDHF) revealed increased intracellular oxidant levels after PEG-ZnPP treatment (Fig. 2). Thus, PEG-ZnPP exerts its cytotoxic effect on tumor cells by inhibiting HO activity, which leads to increased production of toxic oxidants. Reactive oxidants thus formed could trigger the apoptotic pathway (Fig. 3) by activating the caspase-3 cascade, as demonstrated recently for native ZnPP (34). The antiapoptotic role of HO-1 was additionally demonstrated in this study by using siRNA (Fig. 3*B*), which specifically knock down HO-1 expression (Fig. 3*B, inset*) by targeting HO-1 mRNA (26). Among the products of the HO reaction, bilirubin could function as an antioxidant and/or free radical scavenger (10–12). In this context, we found recently that native ZnPP treatment reduced the intracellular bilirubin level and that exogenous bilirubin supplementation could compensate for the cytotoxic effect of ZnPP (34).

Table 1 *Changes in RBC, WBC, hemoglobin, and plasma enzyme levels after PEG-ZnPP treatment of ddY mice*[a]

	RBC ($10^4/\mu$l)	WBC (/μl)	Hb[b] (g/liter)	BUN (mg/dl)	Cr (mg/dl)	AST (IU/liter/at 37°C)	ALT (IU/liter/at 37°C)	LDH (IU/liter/at 37°C)
Control	1074 ± 106.0	8013 ± 862	133.0 ± 13.4	19.7 ± 1.1	0.09 ± 0	249 ± 79.5	37.0 ± 4.4	7611 ± 3221
PEG-PP	1056 ± 50.5	7063 ± 1154	121.3 ± 5.8	17.6 ± 1.8	0.10 ± 0	221 ± 21.6	40.5 ± 5.5	4754 ± 567
PEG-ZnPP	1066 ± 29.8	7983 ± 2902	131.5 ± 7.4	18.2 ± 1.3	0.11 ± 0.01	181 ± 29.7	28.5 ± 1.4	4833 ± 1078

[a] No significant difference was found between each treatment group and the control group in all the selected indices. Values are presented as means ± SE.
[b] Hb, hemoglobin; BUN, blood urea nitrogen; Cr, creatinine; AST, aspartate aminotransferase; ALT, alanine aminotransferase; LDH, lactate dehydrogenase.

As a more important finding, PEG-ZnPP showed marked antitumor activity *in vivo* even after systemic administration to tumor-bearing mice (Fig. 5). In contrast, PEG-PP at the same dose range did not show any antitumor activity. These results correlate well with the findings that PEG-ZnPP, but not PEG-PP, significantly suppressed intratumor HO activity (Fig. 8) and induced apoptosis of tumor cells (Fig. 7). Inhibition of HO activity makes tumor cells susceptible to ROS derived from the metabolism of the cells themselves and ROS derived from the host, *e.g.*, inflammatory cells (18, 19), by reducing the antioxidant bilirubin level. Consequently, tumor cells undergo apoptosis (as seen in Fig. 7) via the caspase-3-dependent pathway, as mentioned above. An anti-inflammatory effect of HO-1 (32, 33) may also be involved in PEG-ZnPP-mediated antitumor activity. CO derived from heme degradation was reported recently to potentially inhibit the production of the proinflammatory cytokine TNF-α from activated macrophages (32, 33). Therefore, inhibition of HO-1 by PEG-ZnPP may enhance the inflammatory response in tumor tissues by increasing TNF-α production, and, hence, reinforce the host defense system. In addition, Yang *et al.* (35) reported that ZnPP induced apoptosis of hamster fibroblasts (HA-1) by up-regulating p53 expression, via ZnPP-mediated Egr-1 binding, which suggests an alternative pathway of ZnPP-induced apoptosis. However, whether this mechanism is involved in the increased apoptosis seen after PEG-ZnPP treatment observed in the present work needs additional investigation.

The antitumor activity of PEG-ZnPP may establish a new role for this compound in cancer treatment. In this regard, targeted delivery of PEG-ZnPP to tumor tissues is critical, because nonspecific distribution of PEG-ZnPP may cause systemic oxidative stress by reducing the antioxidant capacity of normal organs. Although radioactivity derived from ^{65}Zn was detected at the highest level in spleen compared with other organs and tissues (Fig. 4*C*), the HO activity (Fig. 8) and the apoptotic index (Fig. 7) in spleen were unchanged by PEG-ZnPP treatment. These findings suggest that the bioavailability of PEG-ZnPP in the spleen may be limited, probably because of the special histological characteristics of this organ. PEG-ZnPP that accumulates in the spleen may be captured, degraded, or inactivated by the rich RES, including elements such as macrophages, as reported for other macromolecular compounds. This may be the case as well for liver, an organ also rich in RES (29).

In addition, various antioxidative enzymes such as catalase, glutathione peroxidase, and superoxide dismutase may also serve as the protective role against ROS in normal organs; however, these enzymes have been found to be greatly reduced in various tumor cells (36–39), which will increase the vulnerability of tumor cells to ROS. ZnPP is also known to have toxic effects on the bone marrow by inhibiting the growth of erythroid and myeloid cells (30). However, we did not find any significant changes in blood cells after PEG-ZnPP treatment (Table 1). These results, together with those for body weight change (Fig. 6) and the little serum TNF-α production (see "Results"), indicate that systemic side effects of PEG-ZnPP treatment seem to be negligible.

With exception for spleen and liver, PEG-ZnPP preferentially accumulated in solid tumor tissue (Fig. 4*C*). Pharmacokinetic study showed that the amount of PEG-ZnPP in tumor tissue increased in a time-dependent manner (Fig. 4*B*), whereas the amount of PEG-ZnPP in circulation gradually decreased (Fig. 4*A*). This finding suggests that PEG-ZnPP accumulates or is deposited in solid tumor tissues after systemic administration. A similar accumulation of biocompatible macromolecules has been reported for a variety of solid tumor tissues, which may be explained by the unique characteristics of the tumor vasculature (40–44). This phenomenon was named the EPR effect of macromolecules and lipids in solid tumor (40). This EPR effect can be observed for macromolecules having an apparent molecular size larger than 40,000, *i.e.*, large enough to escape from renal clearance (40–44). As expected, the AUC for PEG-ZnPP ($M_r > 70{,}000$ in aqueous medium as a micelle formation; see Ref. 17) showed a 40-fold increase compared with that for native ZnPP ($M_r = 626$; Fig. 4*A*). Thus, PEG-ZnPP is delivered to tumor tissue according to the EPR effect, and, hence, it effectively and selectively inhibits HO activity in tumor.

In conclusion, we demonstrate here that tumor-targeted inhibition of HO activity could be achieved by using the water-soluble HO inhibitor PEG-ZnPP. Inhibition of intratumor HO activity leads to apoptosis of tumor cells by, at least in part, decreasing the bilirubin level, which results in sensitizing tumor cells to oxidative stress. This finding suggests that PEG-ZnPP may intensify the antitumor activity of chemotherapeutics that can produce reactive oxidants and that it may act selectively in the tumor tissue because of the EPR effect. Many chemotherapeutics including conventional antitumor agents such as doxorubicin and camptothecin (45), as well as PEG-conjugated oxidoreductases such as PEG-xanthine oxidase (46) and PEG-D-amino acid oxidase (47), are known to generate ROS and exhibit antitumor effects. The effect of PEG-ZnPP described here is consistent with this antitumor strategy.

ACKNOWLEDGMENTS

We thank Judith B. Gandy for editing this manuscript.

REFERENCES

1. Schacter, B. A. Heme catabolism by heme oxygenase: physiology, regulation, and mechanism of action. Semin. Hematol., *25:* 349–369, 1988.
2. Maines, M. D. Heme oxygenase: function, multiplicity, regulatory mechanisms, and clinical applications. FASEB J., *2:* 2557–2568, 1988.
3. Tenhunen, R., Marver, H. S., and Schmid, R. The enzymatic catabolism of hemoglobin: stimulation of microsomal heme oxygenase by hemin. J. Lab. Clin. Med., *75:* 410–421, 1970.
4. Shibahara, S. Regulation of heme oxygenase gene expression. Semin. Hematol., *25:* 370–376, 1988.
5. Keyse, S. M., and Tyrrell, R. M. Heme oxygenase is the major 32-kDa stress protein induced in human skin fibroblasts by UVA radiation, hydrogen peroxide, and sodium arsenite. Proc. Natl. Acad. Sci. USA, *86:* 99–103, 1989.
6. Mitani, K., Fujita, H., Fukuda, Y., Kappas, A., and Sassa, S. The role of inorganic metals and metalloporphyrins in the induction of haem oxygenase and heat-shock protein 70 in human hepatoma cells. Biochem. J., *290:* 819–825, 1993.
7. Motterlini, R., Foresti, R., Bassi, R., Calabrese, V., Clark, J. E., and Green, C. J. Endothelial heme oxygenase-1 induction by hypoxia. Modulation by inducible nitric oxide synthase and S-nitrosothiols. J. Biol. Chem., *275:* 13613–13620, 2000.
8. Foresti, R., Clark, J. E., Green, C. J., and Motterlini, R. Thiol compounds interact with nitric oxide in regulating heme oxygenase-1 induction in endothelial cells. Involvement of superoxide and peroxynitrite anions. J. Biol. Chem., *272:* 18411–18417, 1997.
9. Doi, K., Akaike, T., Fujii, S., Tanaka, S., Ikebe, N., Beppu, T., Shibahara, S., Ogawa, M., and Maeda, H. Induction of haem oxygenase-1 by nitric oxide and ischaemia in experimental solid tumours and implications for tumour growth. Br. J. Cancer, *80:* 1945–1954, 1999.
10. Farrera, J. A., Jauma, A., Ribo, J. M., Peire, M. A., Parellada, P. P., Roques-Choua, S., Bienvenue, E., and Seta, P. The antioxidant role of bile pigments evaluated by chemical tests. Bioorg. Med. Chem., *2:* 181–185, 1994.
11. Minetti, M., Mallozzi, C., Di Stasi, A. M., and Pietraforte, D. Bilirubin is an effective antioxidant of peroxynitrite-mediated protein oxidation in human blood plasma. Arch. Biochem. Biophys., *352:* 165–174, 1998.
12. Dore, S., Takahashi, M., Ferris, C. D., Zakhary, R., Hester, L. D., Guastella, D., and Snyder, S. H. Bilirubin, formed by activation of heme oxygenase-2, protects neurons against oxidative stress injury. Proc. Natl. Acad. Sci. USA, *96:* 2445–2450, 1999.
13. Petrache, I., Otterbein, L. E., Alam, J., Wiegand, G. W., and Choi, A. M. Heme oxygenase-1 inhibits TNF-α-induced apoptosis in cultured fibroblasts. Am. J. Physiol., *278:* L312–L319, 2000.
14. Otterbein, L. E., Mantell, L. L., and Choi, A. M. Carbon monoxide provides protection against hyperoxic lung injury. Am. J. Physiol., *276:* L688–L694, 1999.
15. Goodman, A. I., Choudhury, M., da Silva, J. L., Schwartzman, M. L., and Abraham, N. G. Overexpression of the heme oxygenase gene in renal cell carcinoma. Proc. Soc. Exp. Biol. Med., *214:* 54–61, 1997.
16. Maines, M. D., and Abrahamsson, P. A. Expression of heme oxygenase-1 (HSP32) in human prostate: normal, hyperplastic, and tumor tissue distribution. Urology, *47:* 727–733, 1996.
17. Sahoo, S. K., Sawa, T., Fang, J., Tanaka, S., Miyamoto, Y., Akaike, T., and Maeda, H. Pegylated zinc protoporphyrin: a water-soluble heme oxygenase inhibitor with tumor-targeting capacity. Bioconjug. Chem., *13:* 1031–1038, 2002.

18. Doi, K., Akaike, T., Horie, H., Noguchi, Y., Fujii, S., Beppu, T., Ogawa, M., and Maeda, H. Excessive production of nitric oxide in rat solid tumor and its implication in rapid tumor growth. Cancer (Phila.), *77:* 1598–1604, 1996.
19. Wu, J., Akaike, T., and Maeda, H. Modulation of enhanced vascular permeability in tumors by a bradykinin antagonist, a cyclooxygenase inhibitor, and a nitric oxide scavenger. Cancer Res., *58:* 159–165, 1998.
20. Drummond, G. S. Control of heme metabolism by synthetic metalloporphyrins. Ann. N. Y. Acad. Sci., *514:* 87–95, 1987.
21. Zalipsky, S. Functionalized poly(ethylene glycol) for preparation of biologically relevant conjugates. Bioconjug. Chem., *6:* 150–165, 1995.
22. Abraham, N. G. Quantitation of heme oxygenase (HO-1) copies in human tissues by competitive RT/PCR. *In:* D. Armstrong (ed.), Methods of Molecular Biology, Vol. 108, pp. 199–209. Totowa, NJ: Humana Press, 1998.
23. Mosmann, T. Rapid colorimetric assay for cellular growth and survival: application to proliferation and cytotoxicity assay. J. Immunol. Methods, *65:* 55–63, 1983.
24. Royall, J. A., and Ischiropoulos, H. Evaluation of 2′, 7′-dichlorofluorescin and dihydrorhodamine 123 as fluorescent probes for intracellular H_2O_2 in cultured endothelial cells. Arch. Biochem. Biophys., *302:* 348–355, 1993.
25. Vermes, I., Haanen, C., Steffens-Nakken, H., and Reutelingsperger, C. A novel assay for apoptosis. Flow cytometric detection of phosphatidylserine expression on early apoptotic cells using fluorescein labeled Annexin V. J. Immunol. Methods, *184:* 39–51, 1995.
26. Elbashir, S. M., Harborth, J., Lendeckel, W., Yalcin, A., Weber, K., and Tuschl, T. Duplexes of 21-nucleotide RNAs mediate RNA interference in cultured mammalian cells. Nature (Lond.), *411:* 494–498, 2001.
27. Hall, R., and Malia, R. G. Basic haematological practice. *In:* R. Hall, and R. G. Malia (eds.), Medical Laboratory Haematology, 2nd ed., pp. 91–94, 101–104. Oxford, England: Butterworth-Heinemann, 1991.
28. Negosecu, A., Lorimier, P., Labat-Moleur, F., Drouet, C., Robert, C., Guillermet, C., Brambilla, C., and Brambilla, E. *In situ* apoptotic cell labeling by the TUNEL method: improvement and evaluation on cell preparations. J. Histochem. Cytochem., *44:* 959–968, 1996.
29. Cassidy, J., Newell, D. R., Wedge, S. R., and Cummings, J. Pharmacokinetics of high molecular weight agents. Cancer Surv., *17:* 315–341, 1993.
30. Lutton, J. D., Abraham, N. G., Drummond, G. S., Levere, R. D., and Kappas, A. Zinc porphyrins: potent inhibitors of hematopoieses in animal and human bone marrow. Proc. Natl. Acad. Sci. USA, *94:* 1432–1436, 1997.
31. Vogt, B. A., Shanley, T. P., Croatt, A., Alam, J., Johnson, K. J., and Nath, K. A. Glomerular inflammation induces resistance to tubular injury in the rat. A novel form of acquired, heme oxygenase-dependent resistance to renal injury. J. Clin. Investig., *98:* 2139–2145, 1996.
32. Otterbein, L. E., Bach, F. H., Alam, J., Soares, M., Tao Lu, H., Wysk, M., Davis, R. J., Flavell, R. A., and Choi, A. M. Carbon monoxide has anti-inflammatory effects involving the mitogen-activated protein kinase pathway. Nat. Med., *6:* 422–427, 2000.
33. Lee, T-S., and Chau, L-Y. Heme oxygenase-1 mediates the anti-inflammatory effect of interleukin-10 in mice. Nat. Med., *8:* 240–246, 2002.
34. Tanaka, S., Akaike, T., Fang, J., Beppu, T., Ogawa, M., Tamura, F., Miyamoto, Y., and Maeda, H. Antiapoptotic effect of haem oxygenase-1 induced by nitric oxide in experimental solid tumor. Br. J. Cancer, *88:* 902–909, 2003.
35. Yang, G., Nguyen, X., Ou, J., Rekulapelli, P., Stevenson, D. K., and Dennery, P. A. Unique effects of zinc protoporphyrin on HO-1 induction and apoptosis. Blood, *97:* 1306–1313, 2001.
36. Greenstein, J. P. Biochemistry of Cancer, Ed. 2, pp. 518–541. New York: Academic Press, 1954.
37. Sato, K., Ito, K., Kohara, H., Yamaguchi, Y., Adachi, K., and Endo, H. Negative regulation of catalase gene expression in hepatoma cells. Mol. Cell. Biol., *12:* 2525–2533, 1992.
38. Hasegawa, Y., Takano, T., Miyauchi, A., Matsuzuka, F., Yoshida, H., Kuma, K., and Amino, N. Decreased expression of glutathione peroxidase mRNA in thyroid anaplastic carcinoma. Cancer Lett., *182:* 69–74, 2002.
39. Yamanaka, N., and Deamer, D. Superoxide dismutase activity in WI-38 cell cultures: effects of age, trypsinization and SV-40 transformation. Physiol. Chem. Phys., *6:* 95–106, 1974.
40. Matsumura, Y., and Maeda, H. A new concept for macromolecular therapeutics in cancer chemotherapy: mechanism of tumoritropic accumulation of proteins and the antitumor agent smancs. Cancer Res., *46:* 6387–6392, 1986.
41. Maeda, H. SMANCS and polymer-conjugated macromolecular drugs: advantages in cancer chemotherapy. Adv. Drug Deliv. Rev., *46:* 169–185, 2001.
42. Maeda, H. The enhanced permeability and retention (EPR) effect in tumor vasculature: the key role of tumor-selective macromolecular drug targeting. Adv. Enzyme Regul., *41:* 189–207, 2001.
43. Maeda, H., Sawa, T., and Konno, T. Mechanism of tumor-targeted delivery of macromolecular drugs, including the EPR effect in solid tumor and clinical overview of the prototype polymeric drug SMANCS. J. Control Release, *74:* 47–61, 2001.
44. Fang, J., Sawa, T., and Maeda, H. Factors and mechanism of "EPR" effect and the enhanced antitumor effects of macromolecular drugs including SMANCS. Adv. Exp. Med. Biol., *519:* 29–49, 2003.
45. Simizu, S., Takada, M., Umezawa, K., and Imoto, M. Requirement of caspase-3 (-like) protease-mediated hydrogen peroxide production for apoptosis induced by various anticancer drugs. J. Biol. Chem., *273:* 26900–26907, 1998.
46. Sawa, T., Wu, J., Akaike, T., and Maeda, H. Tumor-targeting chemotherapy by a xanthine oxidase-polymer conjugate that generates oxygen-free radicals in tumor tissue. Cancer Res., *60:* 666–671, 2000.
47. Fang, J., Sawa, T., Akaike, T., and Maeda, H. Tumor-targeted delivery of polyethylene glycol-conjugated D-amino acid oxidase for antitumor therapy via enzymatic generation of hydrogen peroxide. Cancer Res., *62:* 3138–3143, 2002.